Available online at www.sciencedirect.com
SCIENCE DIRECT®
Journal of Magnetic Resonance 167 (2004) 42–48
JMR Journal of Magnetic Resonance
www.elsevier.com/locate/jmr

Spatially resolved multidimensional NMR spectroscopy within a single scan

Yoav Shrot and Lucio Frydman*

Department of Chemical Physics, Weizmann Institute of Science, Rehovot 76100, Israel

Received 31 July 2003

Abstract

We have recently demonstrated that the spatial encoding of internal nuclear magnetic resonance (NMR) spin interactions can be exploited to collect multidimensional NMR spectra within a single scan. Such experiments rely on an inhomogeneous spatial excitation of the spins throughout the sample, and lead to indirect-domain peaks via a constructive interference among the spatially resolved spin-packets that are thus created. The shape of the resulting indirect-domain echo peaks approaches a Sinc function when the chemical's distribution is uniform, but will depart from this function otherwise. It is hereby shown that a Fourier analysis of either the diagonal- or the cross-peaks resolved in these single-scan two-dimensional (2D) NMR experiments can in fact provide a weighted spatial distribution of the analyte originating such peak, thus opening up the possibility of completing spatially resolved multidimensional NMR measurements within a fraction of a second. Principles of this new mode of analysis are discussed, and examples where the potential of spatially resolved ultrafast 2D NMR spectroscopy is brought to bear are presented. Potential extensions of this approach to higher dimensions are also briefly addressed

Keywords: Magnetic resonance spectroscopy; 2D ^{1}H NMR; Spatial localization; Ultrafast acquisitions; Resolution enhancement

1. Introduction

Nuclear magnetic resonance (NMR) has become a method of choice to carry out a wide variety of in vivo investigations [1,2]. Two main developments combined to endow NMR with this position of preeminence. One was NMR's continuous progress as a magnetic resonance spectroscopy (MRS) tool, where ^{1}H and heteronuclear chemical shifts can be used to identify a variety of metabolic substances. The other came from NMR's incorporation of spatially inhomogeneous magnetic field gradients [3,4], which lead to the advent of magnetic resonance imaging (MRI) techniques enabling the non-invasive localization of healthy and diseased tissues. It thus comes as no surprise that over the last decades numerous hybrid MRS/MRI protocols have been proposed, and shown to lead to unique synergisms for both research and diagnosis [5–8]. Recent studies have revealed that even further insight could be gained by extending the spectroscopic components of these measurements beyond the collection of simple one-dimensional traces [9–11]. This comes again as an expected development, given the dramatic improvements that chemical and biochemical studies experience upon implementing the transition from one- to two-dimensional (2D) forms of NMR spectroscopy [12–14].

In spite of the promise carried by the combination of spatial localization methods with high-dimensional NMR spectroscopy, routine measurements of this kind have been relatively scarce. This is to a large extent a reflection of the relatively long acquisition times that such localized homo- and hetero-nuclear multiD MRS measurements will have associated. Consider for instance a spatially resolved 2D NMR experiment where 32 spectroscopic t_1 points and 16 single-axis imaging voxels are desired; given a repetition delay of 2 s these modest spectral and spatial expectations would lead to data collection times approaching 20 min, an impractical time scale for several in vivo studies. Even longer data acquisition times would result if demanding improvements in the spatial and spectral resolution of the data

* Corresponding author. Fax: +972-8-9344123.
E-mail address: lucio.frydman@weizmann.ac.il (L. Frydman).

1090-7807/$ - see front matter © 2003 Elsevier Inc. All rights reserved.
doi:10.1016/j.jmr.2003.10.008

set, not to mention the inclusion of additional spatial or spectral dimensions.

The purpose of the present study is to demonstrate that, when unbound by signal-to-noise limitations that can only be resolved by extensive signal averaging, hybrid multidimensional/spatially localized MRS/MRI information like the one depicted in the previous paragraph can actually be retrieved within the course of a single data scan. The starting point for this new kind of spatially resolved ultrafast nD NMR experiment lies in the methodology that we have recently introduced for collecting 2D NMR spectra within a single transient [15,16]. The following Section explains how this acquisition methodology coupled to a novel processing protocol enables the collection of spatially resolved NMR data within a sub-second time scale, focusing for simplicity on a case involving two spectral and one spatial dimension. This theoretical analysis is then followed with a series of demonstrations on phantom test samples where 2D NMR spectra arising from compounds placed at different coordinates along a sample's main longitudinal axis can be clearly resolved. Finally, we conclude with a short discussion on additional potential extensions to higher-dimensional spectral and spatial cases.

2. Theory

Ultrafast 2D NMR spectroscopy relies on the paradigm proposed by Jeener, Ernst and co-workers [17,18]

$$Preparation/Excitation - Evolution(t_1) - Mixing - Acquisition(t_2) \quad (1)$$

for implementing 2D NMR experiments and essentially modifies it into the spatially heterogeneous version

$$\begin{bmatrix} Spatially\ selective \\ Preparation/Excitation \end{bmatrix}_{N_1} - \begin{matrix} Position\text{-}dependent \\ Evolution(t_1) \end{matrix} - \begin{matrix} Position\text{-}independent \\ Mixing \end{matrix} - \begin{matrix} Spatially\ resolved \\ Acquisition(t_2). \end{matrix} \quad (2)$$

The purpose of the initial selective excitation process, assumed for simplicity carried out with the aid of a longitudinal G_z gradient applied in an oscillating square-wave manner (Fig. 1), is to create a spatial winding of spin-packets whose pitch will be dictated by the internal spin interaction frequencies. Indeed as a consequence of the selective excitation process a position-dependent evolution will occur during the course of t_1, and originate a winding of spin-coherences defined by discrete evolution phases $\{\phi_j = C\Omega_1(z_j - z_{N_1})\}_{j=0,N_1-1}$. C here is a controllable spatio-temporal constant equal to the ratio between the overall t_1 evolution time and the sample length, and Ω_1 is the particular internal spin interaction that acted over the course of t_1 and which we will eventually want to measure. The winding of spin-packets that has been thus created will be uniformly preserved as either an amplitude or phase modulation throughout the mixing process of the 2D sequence, and then monitored during the course of the spatially resolved acquisition while an oscillating acquisition gradient G_a is applied. Assuming for simplicity that a phase encoding of the spin-packets is preserved throughout the mixing period, the signal that will then be observed for each chemically inequivalent site during the course of the acquisition can be summarized as

$$S(k, t_2) = \left[\sum_{j=0}^{N_1-1} A(z_j) e^{iC\Omega_1(z_j - z_{N_1})} e^{ikz_j} \right] e^{i\Omega_2 t_2}. \quad (3)$$

The $A(z_j)$ coefficients here are amplitudes characterizing the contributions arising from the individual spin-packets into which the sample has been partitioned, to the overall signal voltage detected by the NMR receiver. For a homogeneous cylindrical sample these amplitudes can be simply equated to an overall magnetization signal scaled by the number of excited slices—in essence, a position-independent constant value.[1] The Ω_2 in Eq. (3) represents the internal evolution frequency acting during the course of the t_2 acquisition time and $k = \gamma_a \int_0^t G_a(t')\,dt'$ is a wavenumber associated to the acquisition gradient G_a, which as indicated in Fig. 1 will oscillate numerous (N_2) times during the course of the data acquisition. On inspecting the bracketed expression in this Eq. (1) recognizes a Fourier relation which, when considering a sufficiently large number N_1 of excited slices, will be different from zero only when the k wavenumber fulfills $k \approx -C\Omega_1$.[2] At this point a coherent echo will appear

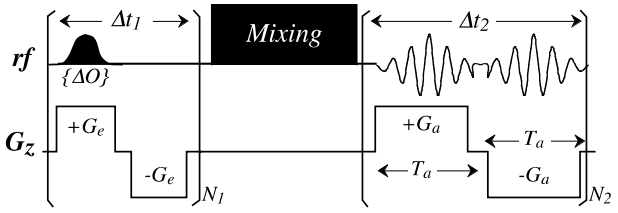

Fig. 1. Generic scheme of an ultrafast 2D NMR pulse sequences based on spatial encoding and decoding processes along the sample's z-axis. The initial excitation encoding the indirect evolution frequencies involves a train of N_1 RF pulses, applied at constant frequency offset increments ΔO and spaced by equal dwell times Δt_1. In combination with a suitable excitation gradient G_e this creates a spatial winding of the evolving spin coherences, which is then preserved throughout the mixing period and onto the beginning of the physical data acquisition time $t_2 = 0$. This winding is then de- and re-coded multiple (N_2) times as a function of t_2 with the aid of an oscillating gradient $\pm G_a$. Following data rearrangement and one-dimensional FT, this allows one to retrieve a complete 2D NMR spectrum within a single scan [15,16].

[1] If RF pulses possessing non-rectangular shapes (e.g., Gaussian) are used for the spins' excitation an additional k dependence will also characterize the $A(z_j)$ coefficients [16]. For the sake of simplicity we shall neglect such enveloping effects throughout this study.

[2] Within $\pm 2n\pi N_1/L$ displacements defining additional "ghost-peaks" [19] which are not of relevance for this study.

mapping the unknown frequency Ω_1 prior to the mixing period, thereby transforming the k axis into an equivalent of the indirect v_1 frequency domain. The direct Ω_2 modulation can be measured conventionally by a 1D Fourier transform (FT) of this data peak as a function of the t_2 variable, leading in this fashion to a 2D NMR resonance at the expected frequency coordinates (Ω_1,Ω_2).

The single-scan 2D NMR approach summarized above appears to be entirely general, and it has been shown susceptible to extensions into higher dimensionalities via the incorporation of additional encoding processes using gradients with different geometries [20]. When considering potential applications of this procedure to MRI or to localized MRS experiments, a possible option that arises includes making one of the frequency axes a spatially encoded one. This implies defining one or several of the evolution frequencies decoded throughout the experiment as $\{\Omega_j = \gamma G_j j\}_{j=x,y,z}$, a procedure whose features and characteristics will be the focus of an independent publication. The aim of the present paper is to examine a different aspect of the localization insight carried by ultrafast 2D NMR acquisitions; namely, the spatial distribution information that resides in *the shape* of the spectroscopic echo peaks that are observed along the indirect k domains. To analyze this localization feature we focus on a particular (Ω_1,Ω_2) peak, and examine the one dimensional line shape that it will exhibit along the k/v_1-axis as a function of the displacement Δk from the $k = -C\Omega_1$ condition. Using the bracketed summation in Eq. (3) as starting point, leads then to

$$S(\Delta k) = \mathrm{e}^{-\mathrm{i}C\Omega_1 z_{N_1}} \sum_{j=0}^{N_1-1} A(z_j)\mathrm{e}^{\mathrm{i}\Delta k z_j}. \tag{4}$$

The $\mathrm{e}^{-\mathrm{i}C\Omega_1 z_{N_1}}$ factor in this equation arises from the non-coincidence assumed between the $z = 0$ sample coordinate and the $t_1 = 0$ condition, and if so desired could be corrected away via an appropriate first-order phase correction. Aside from this artificial factor one recognizes in the $S(\Delta k)$ function a Fourier conjugate of the spins signal amplitudes throughout the sample's z profile. These amplitudes—proportional in turn to the spins' z density weighted by the various spin relaxation processes that might have been active throughout the pulse sequence—can therefore be extracted via a Fourier analysis of the signal's line shape as a function of Δk. For instance when dealing with a homogeneous cylindrical sample and in the absence of spin relaxation, it has been shown that $S(\Delta k)$ will display a Sinc-type dependence [16]; Fourier analysis of this point spread function against Δk will naturally reflect the square sample profile that originated it. In more general cases, a similar ancillary FT(Δk) procedure on each (Ω_1,Ω_2) resonance would allow one to obtain the spatial distribution profile of the spins that lead to the formation of that particular peak. A most appealing aspect of such an approach is that spatially localized information can thus be achieved without really demanding any additions or modifications to the original single-scan 2D NMR spectroscopy experiment. All that is needed is extracting a suitable complex data array defining the full extent of a chosen peak along the k/v_1 axis, and subjecting it to Fourier analysis.

Technical aspects worth discussing are the spatial range and resolution that will characterize this kind of protocols. These will actually follow from the spectral width (SW) characteristics of single-scan 2D NMR experiments; for the basic setup summarized in Fig. 1 and in the preceding paragraph, their values along the indirect and direct domains have been shown given by $SW_1 = |\Delta O(\gamma_a G_a T_a/\gamma_e G_e \Delta t_1)|$, $SW_2 = (2T_a)^{-1}$ respectively. The spatial characteristics that follow from the Fourier analysis of peaks along the k/v_1-domain can be then worked out from coupling these SW considerations to the spectral characteristics of the analyzed metabolites, which will in turn dictate the maximum range of k values that can be used in the FT of any given peak. Indeed assuming that a peak to be Fourier analyzed along the indirect k/v_1-domain is resolved from other peaks along the same axis by a Δv frequency span, will enable data points to be transformed over a maximum range of $\Delta k_{\max} = |\Delta v \gamma_e G_e \Delta t_1/\Delta O|$. For the typical ^{1}H NMR parameters expected in a microscopy setting and at moderate magnetic field strengths ($\Delta v \approx 0.5$ kHz, $\Delta O \approx 5$ kHz, $G_e \approx 10$ G/cm, $\Delta t_1 \approx 1$ ms) this will lead to a spatial resolution in the order of 0.2 cm. The associated field of view will in turn be given by the number of points sampled within each T_a interval; typical dwell time values lead then to spatial fields in the 2–4 cm range. The overall order of magnitude of these two spatial parameters can be expected to increase or decrease by a decade upon switching the experiment to whole-body or microimaging conditions respectively; in either case, this simple analysis reveals that there is an appropriate window of opportunity where both spectral and spatial information can be extracted from single-scan experiments. The following section demonstrates this within a microimaging spectroscopy setting.

3. Results and discussion

In order to test these theoretical predictions, a series of single-scan NMR experiments were carried out on a Bruker Avance 800 MHz NMR spectrometer. The spectrometer's probehead incorporated four frequency channels in an inverse configuration and a triple-axis gradient, even if only the longitudinal z-axis and the ^{1}H channel were used as the sources for the spatial and spectral analyses.[3] Conventional 5 mm NMR tubes were

[3] The high field and sophisticated multi-resonance equipment used in these tests was the result of circumstantial availability, rather than stemming from demands of the experiments themselves.

used to load the experimental samples, and a two-phase spatial heterogeneity was created along these tubes' main axis simply by mixing insoluble organic and aqueous phases. All chemicals and solvents were purchased from Aldrich and used as received; a variety of Matlab 6.5 software programs (The MathWorks) were also written for the sake of reading, processing and simulating the data.

Fig. 2 illustrates how the arguments put forward in the previous section can be used to retrieve both spatial and spectral information, using as example a phantom made up by a water/chloroform mixture. As only a single peak arises from each of these two immiscible phases, a single-scan 2D ^{1}H NMR pulse sequence that actually involved no explicit mixing process was applied as a test. On re-arranging the 1D free-induction decay afforded by such pulse sequence (Fig. 2A) into its proper positions in the $(k/v_1,t_2)$-space and subjecting it to FT(t_2), the expected 2D NMR spectrum composed of two diagonal peaks from the $CHCl_3$ and HDO emerges (Fig. 2B). Extracting then reasonable k-vectors within the neighborhood of the (Ω_1,Ω_2) coordinates characterizing each of these peaks and subjecting these slices to FT against Δk (preceded if so desired by zero-filling) provided then profiles of the z -coordinates occupied by the chemicals originating the 2D NMR peaks, that matched very well our a priori knowledge about their locations (Figs. 2C and D).

The spatially resolved 2D NMR data in Fig. 2 arose from analyses of single-site phases. A slightly different situation is illustrated in Fig. 3, where data were recorded using the lighter, multi-site analyte *n*-butyl chloride as organic phase. Similar profiles are then obtained when the spatial distribution of the organic phase is extracted from any of the *n*-butyl chloride peaks, leading in all cases to results that are complementary to the spatial distribution retrieved from the water resonance (Figs. 3A–E). As a final test of the procedure we illustrate in Fig. 4 another set of single-scan 2D ^{1}H NMR results, recorded this time on the polar compound L-cysteine hydrochloride (8 mg) dissolved in an aqueous phase and coexisting with an organic solution of ethyl acetate (5 μL) dissolved in CCl_4. Unlike in the examples presented so far an isotropic recoupling sequence was incorporated during the course of the mixing [21], leading to the single scan acquisition of a 2D TOCSY NMR spectrum for the two solutes. Cross-peaks in this spectrum were sufficiently resolved to enable a spatial characterization of the analytes' distributions by means of their individual FT(Δk) line shapes; once again, the resulting profiles were as expected for all the diagonal- and cross-peaks chosen for analysis (Fig. 4, bottom).

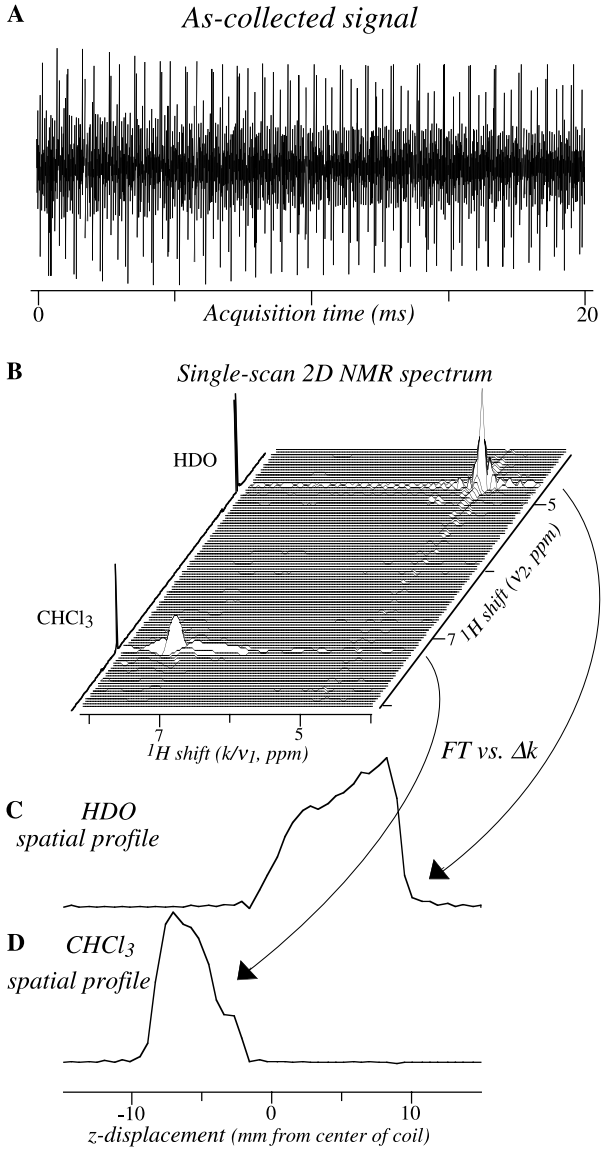

Fig. 2. Summary of events leading to the acquisition of spatially resolved 2D NMR spectra within a single scan. Experiments are illustrated with ^{1}H data recorded on a 5 mm sample tube involving a lower phase of 100% $CHCl_3$, and a top layer made of 12% H_2O in D_2O. Two hundred and fifty microliters aliquots of each phase were employed, with the organic/water interface positioned 2 mm below the center-of-coil z position and the D_2O ^{2}H signal serving as source for B_0 locking and shimming. (A) Time-domain data collected using a pulse sequence like the one illustrated in Fig. 1, but devoid of an actual mixing process. Thirty five square-shaped 150-μs-long RF pulses spaced by $\Delta O = 8$ kHz offsets were employed in the excitation, with G_e a 38 G/cm z gradient. The acquisition involved $N_2 = 64$ gradient echoes with $T_a = 128$ μs and a 32 G/cm gradient. (B) Phase-sensitive 2D stack plot resulting upon rearranging points from the as-collected unidimensional signal ($+G_a$ data only) into their appropriate k and t_2 coordinates, zero-filling the data to 128×128 points, and executing FT(t_2). (C,D) Spatial profiles (magnitude) resulting upon subjecting 25 k-axis points neighboring each of the diagonal peaks in the 2D NMR spectrum, to respective FT(Δk). The spins' distribution arising from this additional analysis is as expected; the tapering-off of the signal intensity visible on approaching the organic/aqueous interface is presumably a result of susceptibility-driven B_0 inhomogeneities, leading to a T_2-weighting of the profiles.

4. Conclusions

It is clear that new avenues in both research and diagnosis could be opened from speeding up the acquisi-

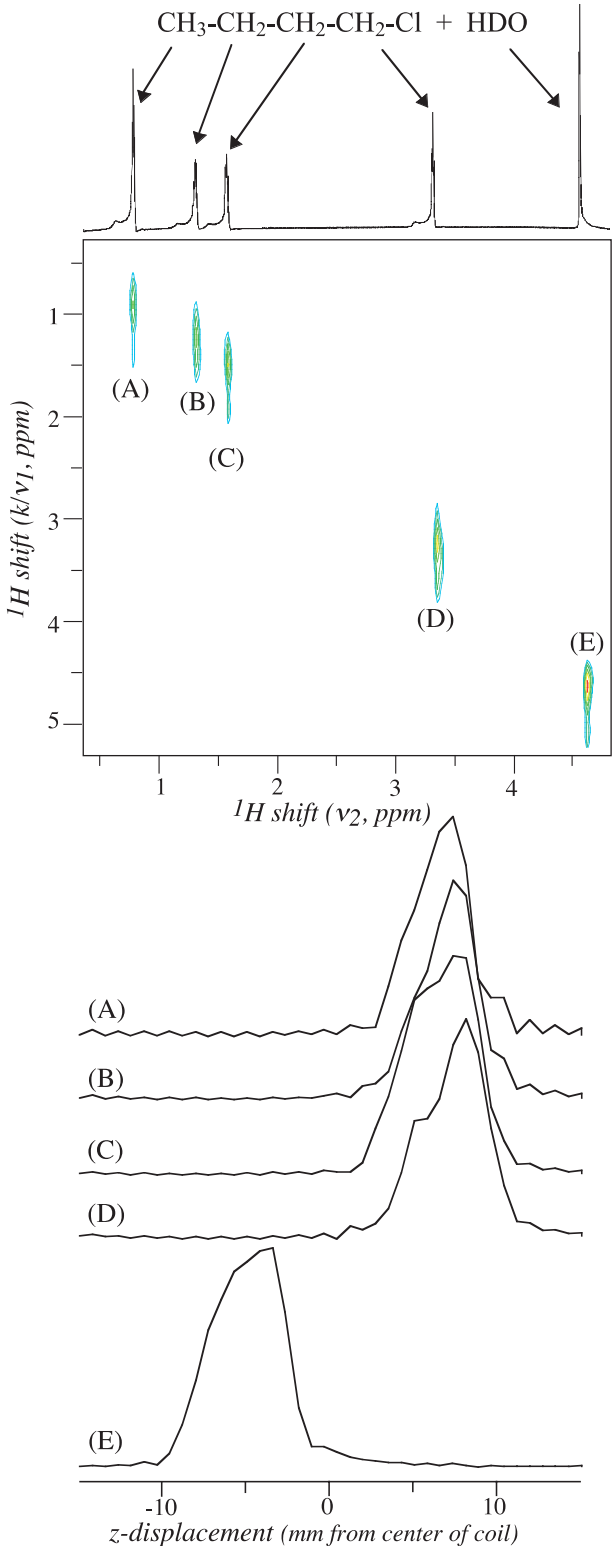

Fig. 3. Idem as Fig. 2 but this time involving the multi-site *n*-butyl chloride analyte as source for the organic layer. Sample considerations and sequence parameters where similar as in Fig. 2, except for pulses that were 100 μs long and $G_a = 40$ G/cm. Shown on top is the single-scan 2D NMR contour plot (magnitude) illustrating the origin of the various diagonal peaks. (A–E) show unidimensional spatial profiles arising from subjecting 20 points neighboring the indicated 2D resonances to zero-filling, FT against Δk, and a magnitude calculation.

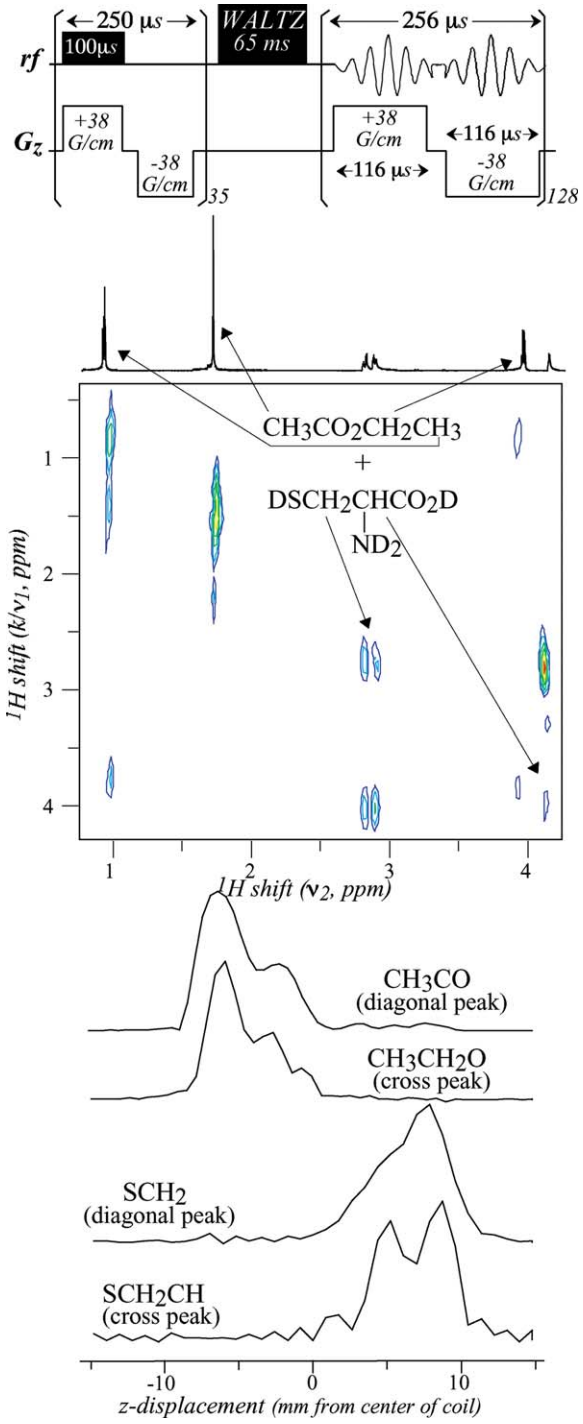

Fig. 4. Spatially resolved ultrafast 2D TOCSY NMR experiment, recorded on polar and non-polar analytes that were mostly dissolved in organic (CCl_4) and aqueous (D_2O) solvents respectively. The pulse sequence employed (top) was essentially as that used to acquire data in Figs. 2 and 3, except for the incorporation of a 65 ms isotropic mixing period and of a 2 s water presaturation pulse (not shown). Suitable data processing lead to the shown 2D contour data plot, where all the expected diagonal and cross-peaks can be identified. Unidimensional spatial profiles resulting on subjecting 20 points neighboring the indicated 2D resonances to an appropriate *k*-axis processing lead to the expected partitioning of the analytes' distributions among organic and aqueous phases (bottom profiles).

tion of spatially localized NMR data. Starting with Mansfield's initial proposition of echo-planar spectroscopic imaging [22], numerous studies where this promise was brought to bear have already been presented [23–26]. Although different strategies to accelerate this kind of acquisitions were then proposed, all these alternatives were based on speeding up the spatial localization rather than the spectroscopic portions of the experiment. This actually appears to be the most competitive approach when dealing with the localized acquisition of one-dimensional MRS spectra. But this may not necessarily be so when having to collect higher-dimensional NMR spectra, where the individual t_i spectroscopy-encoding times would have to be independently incremented. The present study uses an alternative starting point to speed up the acquisition of localized spectroscopic data, as it was the collection of the spectroscopic data components that we strove to compress into a single scan. A simple analysis then shows that spatial localization insight can be obtained as a "fringe benefit" of the ultrafast NMR acquisition mode, without demanding any additions or modifications to the original experiment, or involving extra sensitivity sacrifices. All that is needed is a straightforward post-acquisition processing of the different line shapes observed along the indirect k/v_1 domain. The degree of spatial localization that can be obtained in this manner will be naturally limited by the separation of the peaks arising in the 2D NMR spectrum, yet it is clear that a number of relevant cases will arise where sufficient spatial and spectral degrees of resolution can be accommodated within the same single-scan acquisition.

Accelerated MRS experiments hitherto described in the imaging literature, are usually geared at obtaining unidimensional NMR spectra that appear resolved along at least two spatial dimensions. The spatially resolved ultrafast NMR experiments described in this paper differ from such approaches, in that they end up leading to data sets possessing two spectral plus one spatial dimension. Naturally, now that protocols are available for acquiring both multidimensional NMR spectra as well as multidimensional MRI images within a single scan, hybrid experiments where both approaches are combined for the sake of collecting multidimensional NMR spectra that are also resolved along multiple spatial coordinates could easily become a reality. It should prove feasible for instance to incorporate an additional oscillating gradient into the acquisition segment illustrated in Fig. 1, in order to impose on the spins the extra encoding needed for localizing the 2D NMR data along an independent orthogonal dimension. Yet more intriguing perhaps is the possibility of incorporating these additional orthogonal gradients as part of an accelerated higher-dimensional NMR acquisition, where more than a single spectral axis becomes spatially encoded. Indeed it has been recently shown that the simultaneous use of orthogonal (x,y,z) field gradients can enable the acquisition of 4D NMR spectra within a 10^{-1} s time scale, with peaks along three of the frequency axes arising as a consequence of simultaneous constructive interferences among spin packets while peaks along the fourth axis become conventionally unraveled via FT as a function of the t_4 acquisition time [20]. In such cases, a Fourier analysis procedure similar to the one described in the present manuscript but implemented along the various $\{k_\alpha/v_i\}_{\alpha/i=x/1,y/2,z/3}$ dimensions could provide a full location on the spatial position of an analyte originating a peaks—in essence a seven-dimensional single-scan NMR set incorporating 4D MRS with independent 3D MRI localization. This might be more than what is warranted for a majority of practical applications; still, these various possibilities and their potential applications are worth considering and will be further discussed in a future study.

Acknowledgments

This work was supported by the Philip M. Klutznick Fund for Research, by the Minerva Foundation (Munich, FRG), as well as by a grant from the Henry Gutwirth Fund for the Promotion of Research.

References

[1] D.M. Grant, R.K. Harris (Eds.), Encyclopedia of NMR, Wiley, Chichester, 1996.
[2] M.A. Brown, R.C. Semelka, MRI: Basic Principles and Applications, Wiley–Liss, New York, 1999.
[3] P.C. Lauterbur, Nature 242 (1973) 190.
[4] P. Mansfield, P.K. Grannell, J. Phys. C 6 (1973) 422.
[5] T. Brown, B. Kincaid, K. Ugurbil, Proc. Natl. Acad. Sci. USA 79 (1982) 3523.
[6] I. Pykett, B. Rosen, Radiology 149 (1983).
[7] W.T. Dixon, Radiology 153 (1984) 189.
[8] N. Salibi, M.A. Brown, Clinical MR spectroscopy: First principles, Wiley–Liss, New York, 1998.
[9] L.N. Ryner, J.A. Sorenson, M.A. Thomas, J. Magn. Reson. B 107 (1995) 126.
[10] A. Ziegler, A. Metzler, W. Kockenberger, M. Izquierdo, E. Komor, A. Haase, M. Décorps, M. vonKienlin, J. Magn. Reson. B 112 (1996) 141.
[11] M.A. Thomas, K. Yue, N. Binesh, P. Davanzo, A.K. A, B. Siegel, M. Frye, J. Curran, R. Lufkin, P. Martin, B. Guze, Magn. Reson. Med. 46 (2001) 58.
[12] K. Wuthrich, NMR of Proteins and Nucleic Acids, Wiley, New York, 1986.
[13] R.R. Ernst, G. Bodenhausen, A. Wokaun, Principles of Nuclear Magnetic Resonance in One and Two Dimensions, Clarendon Press, Oxford, 1987.
[14] J. Cavanagh, W.J. Fairbrother, A.G. Palmer III, N.J. Skelton, Protein NMR Spectroscopy: Principles and Practice, Academic Press, San Diego, 1996.
[15] L. Frydman, T. Scherf, A. Lupulescu, Proc. Natl. Acad. Sci. USA 99 (2002) 15858.

[16] L. Frydman, T. Scherf, A. Lupulescu, J. Am. Chem. Soc. 125 (2003) 9204.
[17] J. Jeener, Ampere International Summer School II, Basko Polje, Yugoslavia, 1971.
[18] W.P. Aue, E. Bartholdi, R.R. Ernst, J. Chem. Phys. 64 (1976) 2229.
[19] Y. Shrot, L. Frydman, J. Magn. Reson. 164 (2003) 351.
[20] Y. Shrot, L. Frydman, J. Am. Chem. Soc. 125 (2003) 11385.
[21] L. Braunschweiler, R.R. Ernst, J. Magn. Reson 53 (1983) 521.
[22] P. Mansfield, Magn. Reson. Med. 1 (1984) 370.
[23] S. Matsui, K. Sekihara, H. Kohno, J. Am. Chem. Soc. 107 (1985) 2817.
[24] P.M. Jakob, F. Kober, R. Pohman, A. Haase, J. Magn. Reson. B 110 (1996) 278.
[25] E. Adalsteinsson, D.M. Spielman, Magn. Reson. Med. 41 (1999) 8.
[26] R.V. Mulkern, L.P. Panych, Concepts Magn. Reson. 13 (2001) 213.